Heterogeneous self-assembly of cells on DNA micro-patterns for arbitrary-defined cellular networks

Hiroaki Onoe, Sonny C. Hsiao, Erik S. Douglas, Zev J. Gartner,
Carolyn R. Bertozzi, Matthew B. Francis, and Richard A. Mathies

Supporting Information

PMMA protection layer for ssDNA patterns on a glass substrate.

We examined the effect of a PMMA protection layer on ssDNA spots for the cell capture. Experimental summaries are shown in Figure S1(a). Exp. #1 is a normal protocol for the cell capture that is written in Experimental Section: NH_2-DNA spots (Sequence A) were created on an aldehyde glass with reductive amination. Jurkat cells were modified with NHS-DNA (Sequence A') and stained with CellTracker Blue. In Exp. #2, the NH_2-DNA spots were covered with a PMMA layer by spin coating at 2500 rpm for 30 s. S-1818 photoresist was then spun on the PMMA layer at 500 rpm for 10 s and 2500 rpm for 30 s, followed by 120 °C bake for 2 min. After that, the PMMA and S-1818 photoresist layers were removed with acetone. We repeated this coating and removing process three times. Then, cell capture was performed on both spots (Exp. #1 and #2) as the same manner as in Experimental Section. In both experiments, there is no significant difference in the cell capture density (Figure S1(b)(c)). This result shows that coating and removing procedures of the PMMA/PR layers do not damage the immobilized ssDNA for the cell capture.

Next, we checked the degradation of the ssDNA covered with the PMMA layer. Experimental flows are shown in Figure S2(a). In Exp. #1 (control), NH_2-DNA (Sequcne A) was immobilized on an aldehyde glass as the same manner as the Experimental Section, and stored in the air at room temperature for 4 days before cell capture. In Exp. #2, immobilized NH_2-DNA spots were covered with PMMA and S-1818 layers as the same procedure in Figure S1. The buried NH_2-DNA was stored in the air at room temperature for 4 days. The PMMA and S-1818 layers were removed with acetone before cell capture. In Exp. #3, PMMA and S1818 layers were coated on NH_2-DNA spots, and removed with acetone immediately. The DNA spots were then stored in the air at room temperature for 4 days. Cell capture (Jurkat cells with A' sequence) was performed on all of the DNA spots (Exp. #1-#3) as the same manner in Experimental Section. Images of the captured Jurkat in Exp. #1-#3 and their capture densities are shown in Figure S2(b) and (c), respectively. The capture density in Exp. #2 was smaller (~0.6) than those of the other two experiments (~1.0 in both Exp. #1 and #2). This result shows that the DNA in the PMMA layer is slowly degraded at the time scale of several days and it causes low cell capture density.

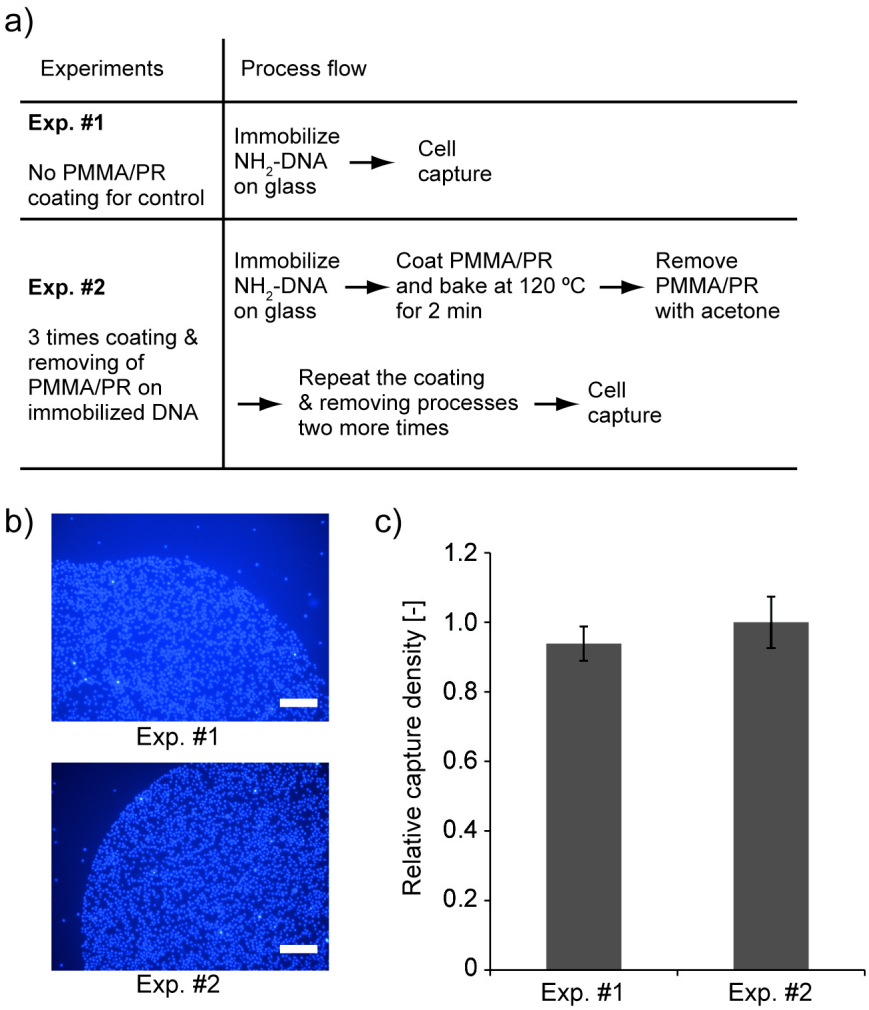

Figure S1. Comparison between standard DNA cell capture (**Exp. 1** for control) and cell capture after PMMA/PR coat and removal (**Exp. 2**). **a)** Experimental procedures. DNA-NH_2 (sequence A) was spotted on an aldehyde glass and immobilized by reductive amination. In Exp. 2, PMMA/PR layers were spincoated on the immobilized DNA molecules, and then removed with acetone. Jurkat cells were modified with NHS-DNA (sequence A'), and then captured on the DNA spots. **b)** Fluorescent images of captured Jurkat cells and **c)** their capture densities on each experiment. Error bars represent the standard deviation of 4 replicate experiments.

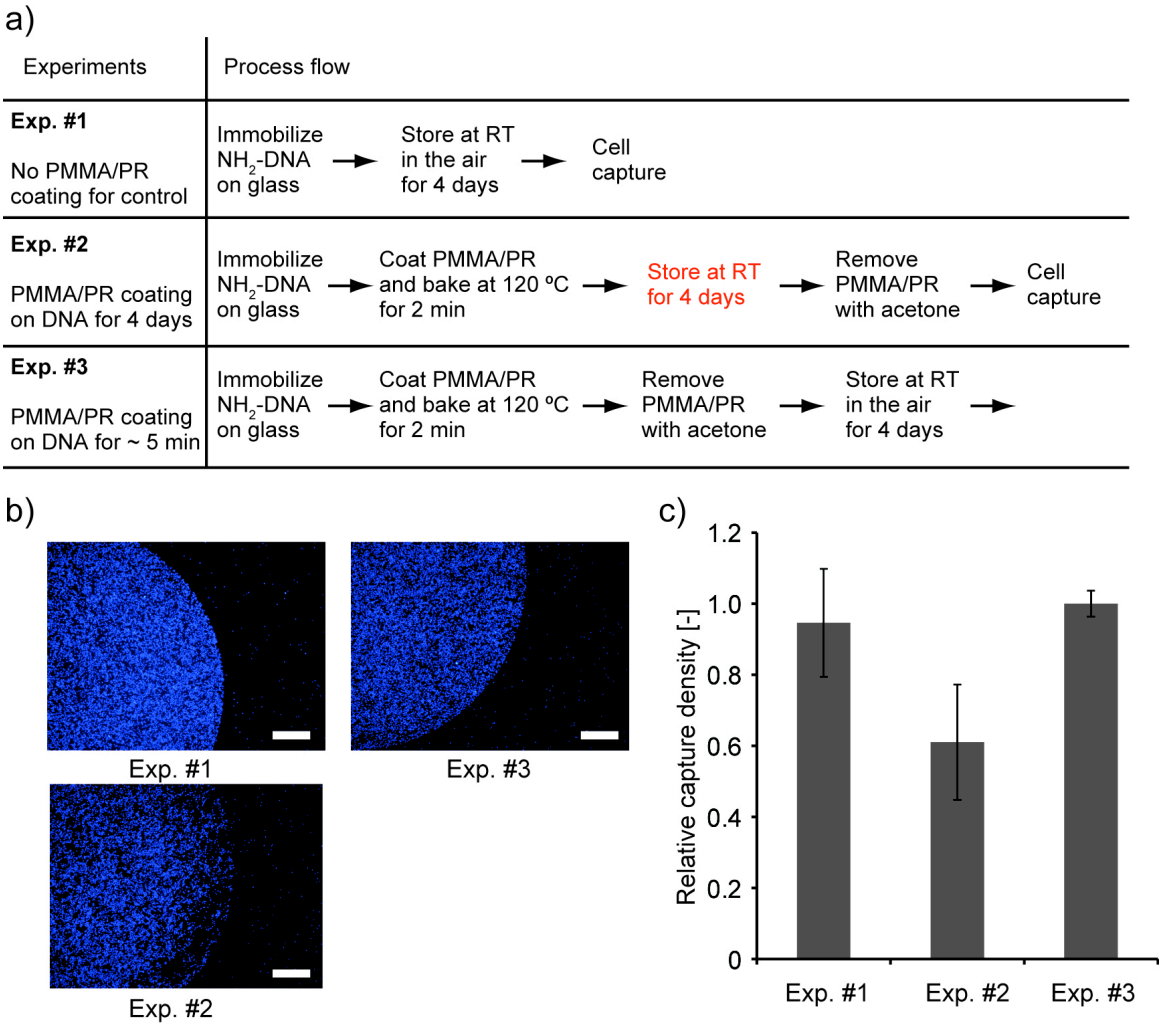

Figure S2. Degradation of immobilized DNA molecules buried in a PMMA layer. **a)** Experimental procedures. DNA-NH_2 (sequence A) was spotted on an aldehyde glass and immobilized by reductive amination. In Exp. #1 (for control), the DNA-immobilized glass was left in the air for 4 days. In Exp. #2, PMMA and PR layers were spincoated on the immobilized DNA spot, and then left for 4 days while the DNA was buried in the PMMA layer. After that, the PMMA and PR layers were removed with acetone. In Exp. #3, the spotted DNA was left in the air for 4 days after coating and removing the PMMA and PR layers. For all experiments, Jurkat cells were modified with NHS-DNA (sequence A') and stained with CellTracker Blue, and then captured on the DNA spots. **b)** Fluorescent images of captured Jurkat cells and **c)** their capture densities on each experiment. Error bars represent the standard deviation of 4 replicate experiments.

IL-3-dependent growth rate of FL-5.12 cells.

To examine IL-3-dependent growth rate of FL-5.12 cells, we cultured FL-5.12 cells in media with various IL-3 concentrations. We used RPMI-1640 media with 10 % FBS and 1 % P/S containing 0, 0.07, 0.55, 4.4, or 35 pg/ml murine recombinant IL-3 (Sigma) for the experiment. FL-5.12 cells (25 x 10^4 cells/ml) were cultured in each medium for 96 h at 37 ^{o}C in 5% CO_2 environment. After that, the cultured cells were counted to evaluate the growth ratio, (number of cells after 96 h of culture)/(number of cells before culture). Figure S3(a) and (b) show the IL-3-dependent proliferation of the FL-5.12 cells. The number of the proliferated FL-5.12 cells increases as the IL-3 concentration increases.

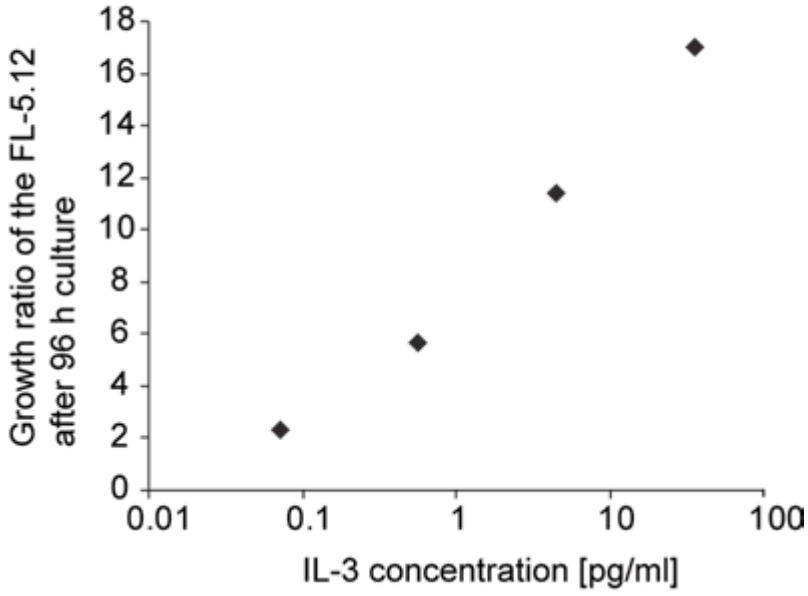

Figure S3. Proliferation of FL-5.12 cells in various concentration of IL-3 in a culture medium. The growth ratio is shown (live cells at 96 h vs. initial cells at t=0) for the FL-5.12 cells vs. the IL-3 concentration of the medium. Specific IL-3 concentrations screened were 35, 4.4, 0.55, 0.07 and 0 pg/mL. The speed of the FL-5.12 proliferation increases as the IL-3 concentration increases.

Images of the cultured cell patterns for (i) FL-5.12 and CHO cells, and (ii) FL-5.12 and CHO IL-3 cells with anti IL-3 antibodies.

Figure S4 shows that superimposed images of the patterned (a) FL-5.12 and CHO cells, and (b) FL-5.12 and CHO IL-3 cells with anti-IL-3 antibodies. In Figure S4(a), almost all the patterned FL-5.12 cells disappeared after 72 h of culture since the co-cultured CHO cells does not produce IL-3 molecules. In contrast, the CHO cells at the center proliferated well after 72 hours. Similarly in Figure S4(b), most of the patterned FL-5.12 cells died after 72 h of culture, since IL-3 molecules that were produce by the CHO IL-3 cells were blocked with anti IL-3 antibody in the agarose.

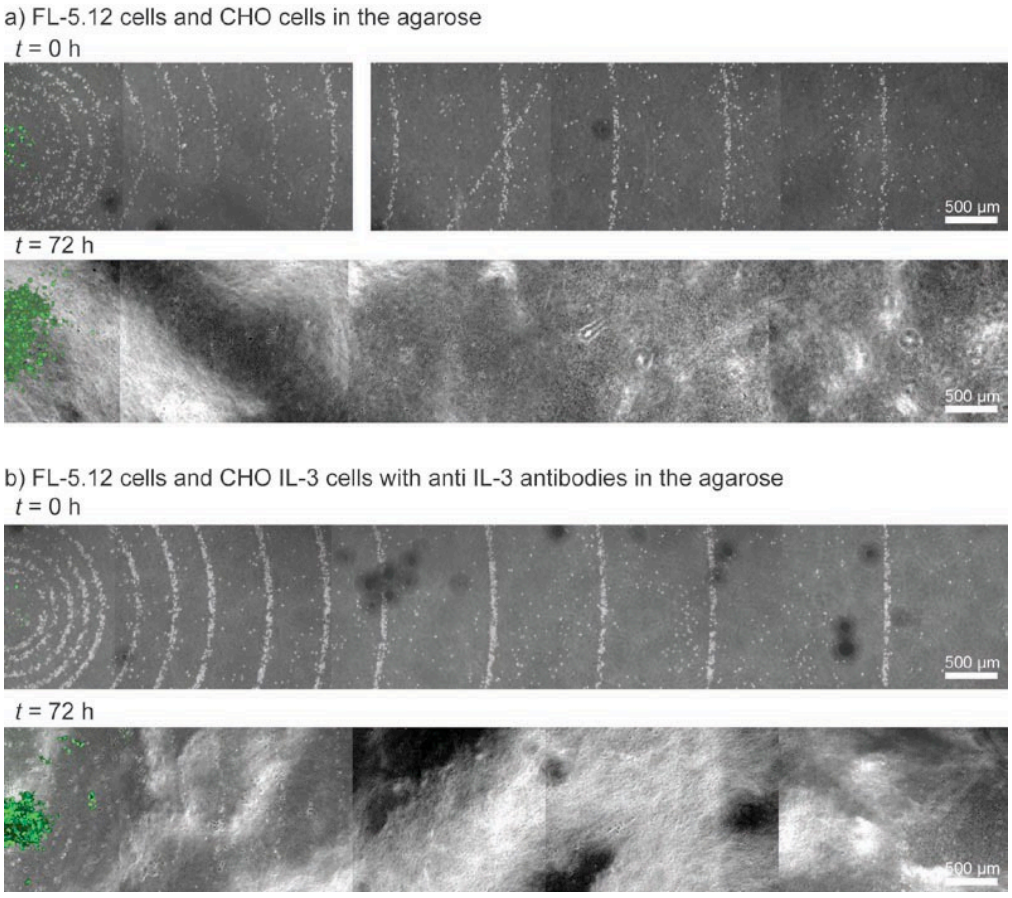

Figure S4. Microscopic images of FL-5.12 and CHO cells in medium-containing agarose (a), and FL-5.12 cells and CHO IL-3 cells in the agarose with anti IL-3 antibody (b).

Calculation of diffusion speed of IL-3 molecules in agarose gel.

The diffusion coefficient of protein molecules in hydrogel, D_{gel}, can be calculated by the following formula:[1]

$$\frac{D_{gel}}{D_{solution}} = \exp(-\phi^{\frac{1}{2}} \frac{r_H}{r_f}) \qquad (1)$$

where $D_{solution}$ is diffusion coefficient of protein in solution, ϕ is volume fraction of agarose, and r_H is hydrodynamic radius, and r_f is average fiber radius of agarose. $D_{solution}$ and ϕ are expressed as

$$D_{water} = \frac{k_B \cdot T}{6\pi\eta \cdot r_H}, \qquad (2)$$

$$\text{and} \quad \phi = c_{agarose} / (\rho_{agarose} \cdot \omega_{agarose}), \qquad (3)$$

respectively, where k_B is Boltzmann constant, T is temperature, η is solvent viscosity, $c_{agarose}$ is concentration of the agarose in the gel, $\rho_{agarose}$ is agarose density, and $\omega_{agarose}$ is mass fraction of agarose in a fiber.[1]

With these equations (1)-(3), diffusion coefficient of IL-3 molecules in 1 % agarose hydrogel at 37 ^{o}C is calculated to be 1.576 x 10^{-10} $m^2 \cdot s^{-1}$, where r_H is 1.89 nm for IL-3 molecules (15.1 KDa), r_f is 1.89 nm,[2] η is 6.91 x 10^{-4} Pa·s, T is 310 K, $c_{agarose}$ is 0.01, $\rho_{agarose}$ is 1.64 $g \cdot ml^{-1}$,[1] and $\omega_{agarose}$ is 0.625.[1]

The root square mean displacement of molecules in two dimensions, x, is express as a function of time, t, as

$$t = \frac{x^2}{4D}, \qquad (4)$$

where n is dimension of the system, and D is diffusion coefficient.[3, 4] Therefore, approximate travel speed, x/t, for IL-3 molecules in 1% agarose at 37 ^{o}C is estimated to be ~1.5 mm/hour in our diffusion-based cell communication experiment.

Concentration gradient of IL-3 molecules in agarose gel.

Francis and Palsson suggested a model for calculating a concentration of cyto/chemokine signaling molecules from a single cell as a function of spatial location and time [5]. We applied this model to our IL-3 cell communication experiment to estimate the special distribution of the produced IL-3 molecules from the patterned CHO IL-3. To simplify the calculation, we assume that (i) the IL-3 production rate by the CHO IL-3 cells is constant during the experiment and (ii) the IL-3 molecules are completely diluted at very far from the center.

We define that the IL-3 production rate from all of the patterned CHO IL-3 cells, F_0 (molecules/area·time), is an amount of IL-3 molecules per unit area on the upper hemisphere above the CHO IL-3 pattern as illustrated in Figure S5(a). Thus, F_0 is calculated to be 1.49 x 10^{-9} $pg \cdot \mu m^{-2} \cdot s^{-1}$ as,

$$F_0 = A_{\text{IL-3}} \cdot N / 2\pi \cdot r^2, \qquad (5)$$

where $A_{\text{IL-3}}$ is the average IL-3 production rate of the single CHO IL-3 cell ($A_{\text{IL-3}}$ = 3.9 x 10^{-6} pg·s^{-1}), N is the number of the CHO IL-3 cells on the pattern (N = 150), and r is the radius of the pattern (r = 250 μm) in our experiment.

Using this value, concentration of IL-3 molecules, c, can be estimated as a function of distance from the center, d, and time, t, as follows: [5]

$$c(d,t) = \frac{F_0 r}{2Dd}\sqrt{\frac{4Dt}{\pi}}\left\{ e^{\frac{-(d-r)^2}{4Dt}} - e^{\frac{-(d+r)^2}{4Dt}} - \frac{|d-r|}{\sqrt{\frac{4Dt}{\pi}}} erfc\left(\frac{|d-r|}{\sqrt{4Dt}}\right) + \frac{|d+r|}{\sqrt{\frac{4Dt}{\pi}}} erfc\left(\frac{|d+r|}{\sqrt{4Dt}}\right) \right\} \qquad (6)$$

where D is the diffusion coefficient of the IL-3 molecules and *erfc* is the complementary error function. According to the equation (6), the relationship between the IL-3 concentration, c, and the distance, d, is plotted in Figure S5(b). The plot indicates that the IL-3 concentration gradient is generated during 72 hours of culture, and this gradient causes the distance-dependent growth of the FL-5.12 cells shown in Figure 6. The ratios of the IL-3 concentration at R1 to R15, at R9 to R15, and at R13 to R15 are shown in Figure S5(c). Note that c(Rx) means the concentration of the IL-3 at ring pattern Rx. This result indicates that the FL-5.12 cells on the most inner R1 pattern have more than ~70 times higher IL-3 concentration than that on the most outer R15 pattern during the experiment. In the cases of the FL-5.12 cells on R9 and R13, the ratios of the IL-3 concentration to R15 are more than ~8 and ~2.5, respectively.

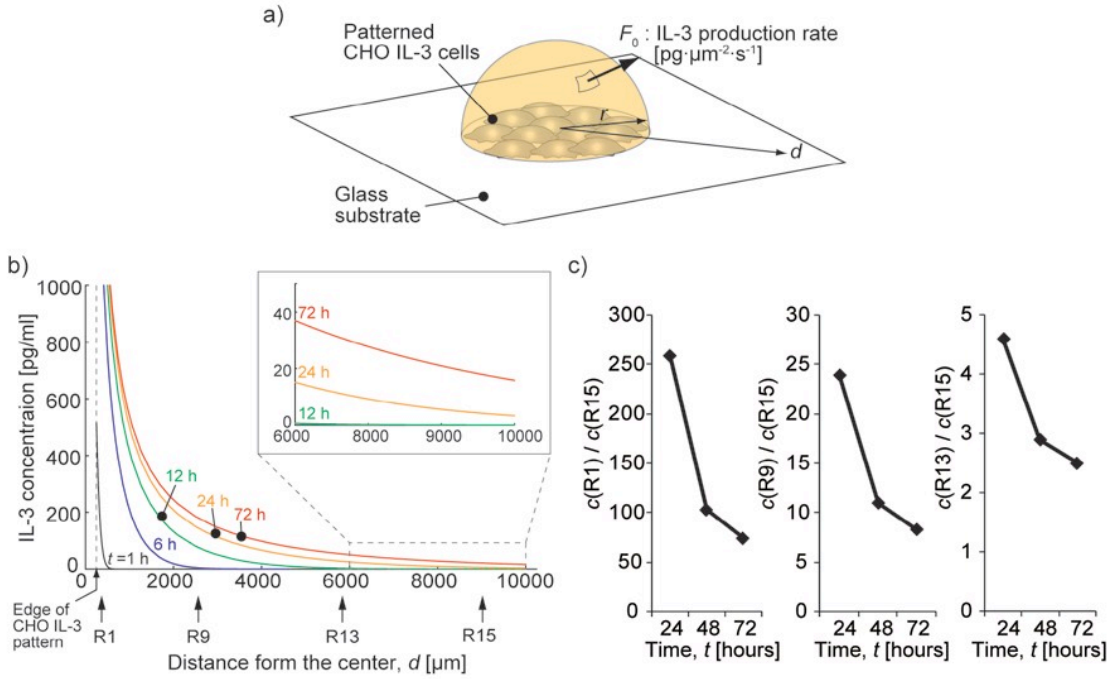

Figure S5. Concentration gradient of IL-3 molecules in agarose gel **a)** A calculation model of the total IL-3 production rate from the patterned CHO IL-3 cells. **b)** The calculated concentration gradient of the IL-3 molecules. **c)** The ratio of the IL-3 concentration at R1 to R15 (c(R1)/c(R15)), R9 to R15 (c(R9)/c(R15)), and R13 to R15 (c(R13)/c(R15)) during the experiment, where c(Rx) means that IL-3 concentration at ring pattern Rx.

References

[1] A. Pluen, P. A. Netti, R. K. Jain, D. A. Berk Diffusion of Macromolecules in Agarose Gels: Comparison of Linear and Globular Configurations. *Biophysical Journal* **1999**, *77*, 542.

[2] E. M. Johnson, D. A. Berk, R. K. Jain, W. M. Deen Hindered diffusion in agarose gels: test of effective medium model. *Biophysical Journal* **1996**, *70*, 1017.

[3] H. C. Berg *Random walks in biology*, Princeton University Press, **1993**.

[4] M. Mayer, J. Yang, I. Gitlin, D. H. Gracias, G. M. Whitesides Micropatterned agarose gels for stamping arrays of proteins and gradients of proteins. *Proteomics* **2004**, *4*, 2366.

[5] K. Francis, B. O. Palsson Effective intercellular communication distances are determined by the relative time constants for cyto/chemokine secretion and diffusion. *Proc. Nat. Acad. Sci. USA* **1997**, *94*, 12258.